Individualized Gait Generation for Rehabilitation Robots Based on Recurrent Neural Networks

Zikang Zhou, Binghong Liang, Guowei Huang, Biao Liu, Jinjin Nong, and Longhan Xie, *Member, IEEE*,

***Abstract*—Individualized reference gait patterns for lower limb rehabilitation robots can greatly improve the effectiveness of rehabilitation. However, previous methods can only generate customized gait patterns at several fixed discrete walking speeds and generating gaits at continuously varying speeds and stride lengths remains unsolved. This work proposes an individualized gait pattern generation method based on a recurrent neural network (RNN), which is proficient in series modeling. We collected the largest gait data set of this kind, which consists of 4,425 gait patterns from 137 subjects. Using this data set, we trained an RNN to create a function mapping from body parameters and gait parameters to a gait pattern. The experimental results indicate that our model is able to generate gait patterns at continuously varying walking speeds and stride lengths while also reducing the errors in the ankle, knee, and hip measurements by 12.83%, 20.95%, and 28.25%, respectively, compared to previous state-of-the-art method.**

***Index Terms*—Gait rehabilitation, gait generation, recurrent neural network.**

I. Introduction

ROBOTIC systems are gaining popularity as rehabilitation tools for patients with impaired mobility; for instance, patients with hemiplegia caused by a stroke [1] or paraplegia caused by a spinal cord injury [2]. Numerous lower limb rehabilitation robots (LLRRs), such as LOPES [3], ALEX [4], WalkTrainer [5], Lokomat [6], and MINDWALKER [7] have been reported to be clinically effective. These robots help patients restore mobility by assisting them in performing rehabilitation tasks such as walking and cycling intensively. Many studies have proven that these repetitive activities are helpful for the recovery of motor abilities [8], [9].

Manuscript received September 28, 2020; revised December 3, 2020; accepted December 6, 2020. Date of publication December 17, 2020; date of current version March 1, 2021. This work was supported in part by the National Natural Science Foundation of China under Grant 52075177; in part by the Joint Fund of the Ministry of Education for Equipment Pre-Research under Grant 6141A02033124; in part by the Research Foundation of Guangdong Province under Grant 2019A050505001 and Grant 2018KZDXM002; in part by the Guangzhou Research Foundation under Grant 202002030324 and Grant 201903010028, in part by the Zhongshan Research Foundation under Grant 2020B2020; and in part by the Shenzhen Institute of Artificial Intelligence and Robotics for Society under Grant AC01202005011. *(Corresponding author: Longhan Xie.)*

The authors are with the Shien-Ming Wu School of Intelligent Engineering, South China University of Technology, Guangzhou 510640, China (e-mail: mezikang@mail.scut.edu.cn; 2498675802@qq.com; 616126836@qq.com; 437147672@qq.com; 591265029@qq.com; melhxie@scut.edu.cn).

Digital Object Identifier 10.1109/TNSRE.2020.3045425

Although much progress has been made in the field of LLRRs, it remains a challenge to adapt LLRRs to different users' gait patterns. Research shows that each person has a unique gait pattern [10], which is often highly related to physical body parameters, such as height, weight, and gender, and gait parameters, such as walking speed and stride length [11], [12]. Vallery *et al.* have proved that customized gait trajectories for rehabilitation robots can improve the efficiency of the rehabilitation [13]. Many works attempt to generate a customized gait for users of LLRRs based on body parameters and target gait parameters; generally, they can be divided into model-based methods and learning-based methods.

Model-based optimization methods attempt to model and simulate human walking by hypothesizing a mathematical human-skeleton model and cost functions for the human walking process; they calculate the optimized limb motions subject to a minimum cost function value. In [14], Anderson *et al.* modeled the human body as a 23 degrees-of-freedom (DOFs) mechanical linkage driven by 54 muscles. The optimization problem calculates the muscle forces and limb motions that minimize metabolic energy. Xiang *et al.* created a skeletal model that has 38 active DOFs, predicting human gait both in a symmetric [15] and asymmetric way [16] by minimizing the dynamic effort of walking while considering the associated physical and kinematical constraints.

However, for all of these model-based methods [14]–[16], whether the optimization result is reasonable depends on the degree of similarity between the virtual human model and the real human body, and regardless of how elaborate the model is, it cannot fully describe the real human body. In addition, the optimization processes are highly sensitive to the boundary conditions and the mass-inertial parameters, and are prone to numerical instabilities.

Recently, with the rapid development of machine learning techniques, researchers have turned to learning-based methods, considering gait generation as a regression problem [17]–[21]. Typically, these works collect a database of healthy people, which contains the gait patterns of many subjects walking in various states and their body parameters. Then they use a regression model to establish a mapping relationship between body parameters and gait patterns, and a personalized gait pattern can be obtained when the patient's body parameters are fed into the trained regression model.

Artificial neural networks are great tools for regression. Lim *et al.* used a Multi-Layer Perceptron Neural Network (MLPNN) [17], Luu *et al.* used Generalized Regression Neural

Networks (GRNNs) [19] to predict gait patterns from a subject's body and gait parameters. Gait patterns are represented by Fourier coefficients; in this way, the output dimensions and required model complexity are reduced. However, this inevitably introduces reconstruction errors.

Yun *et al.* [18], Wu *et al.* [20], and Hong *et al.* [21] utilized Gaussian Process Regression (GPR) to create a mapping from body parameters to gait patterns. Since their data sets contain only gait patterns at discrete fixed values of walking speeds, their performance is bound to be unsatisfactory when self-paced walking is needed. In addition, Hong *et al.* [21] utilized the Gaussian Process Dynamic Model (GPDM) as a nonlinear dimensionality reduction technique to represent gait patterns. Nevertheless, modeling gait patterns with GPDM causes an error up to 20%.

Another research direction of learning-based gait generation is to infer abnormal joint motion from normal joint motion. Liu *et al.* [22] employed a Deep Spatial-Temporal Model to generate the trajectory of an ill-functioning knee based on other normal joint motions. Nevertheless, they did not consider the body characteristics of the subject, which have a tremendous influence on gait patterns. In addition, the movement of the healthy side of patients with hemiplegia is affected by the motion of the affected side [23], so if this method is to be introduced into the recovery of hemiplegia gait, methods to eliminate this effect need to be considered.

None of the previous methods are able to generate gait at continuously varying walking speeds and stride lengths, which limits the rehabilitation effect. Walking speed and stride length are two significant gait parameters that greatly affect walking kinematics and kinetics [11], [24]–[26]. Varying walking speed is needed in different stages of gait rehabilitation. For example, patients with poor motor ability need to walk at a slower pace, while those in better condition need to walk at a faster pace to achieve a better training effect. Stride length and walking speed also have great effects on walking stability. Espy *et al.* [25] showed that a smaller stride length improves stability against falls, whereas a smaller walking speed does the opposite. Thus, generating gait patterns at continuously varying speeds and strides is important, but all previous methods have failed to do so.

The major contribution of this paper is a learning-based individualized gait generation method based on Recurrent Neural Networks (RNNs) aimed at generating reference motions for gait rehabilitation robots. We collected the largest gait data set to the best of knowledge, which consists of 4,425 gait patterns at self-designated walking speeds and strides of 137 subjects and their body parameters. Then, we created RNNs to map body parameters and gait parameters to gait patterns. After the RNNs were trained using the data set, they are able to generate reference gait patterns for a specific subject at a specific walking speed and stride length. Experimental results indicate that our model is able to generate gait patterns with continuously varying walking speeds and stride lengths, which all previous works failed to achieve. We also offer a comparison of prediction errors between our method and previous methods as a validation of the advantages of our method.

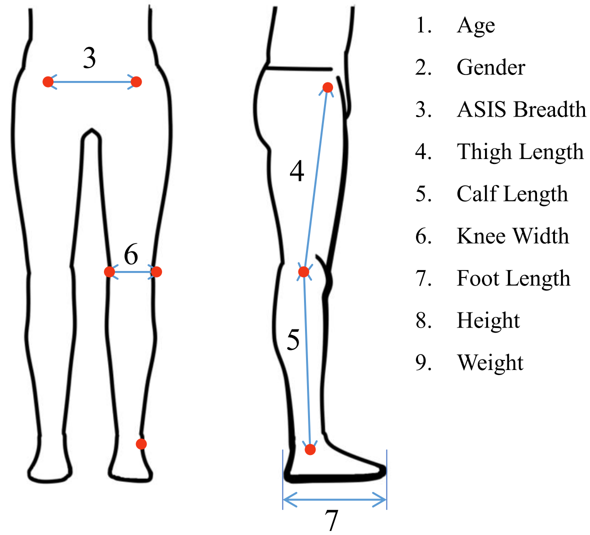

Fig. 1. Definition of the collected body parameters. ASIS is an abbreviation for the anterior superior iliac spine. The knee landmark (KL) is the point at which the rotation axis of the knee intersects with the outer skin, and the ankle landmark (AL) is the point at which the rotation axis of the ankle intersects with the outer skin. Thigh length is defined as the distance between the ASIS and KL, and calf length is the distance between the KL and AL.

TABLE I
MEAN AND STANDARD DEVIATION OF THE COLLECTED BODY PARAMETERS FROM 137 EXPERIMENT PARTICIPANTS[1]

Index	Parameter	Mean	Std	Max	Min	Unit
1	Age	20.64	1.81	29	17	year
2	Gender	n/a	n/a	n/a	n/a	n/a
3	ASIS breadth	241.99	18.37	290	205	mm
4	Thigh length	461.96	26.20	544.5	397.5	mm
5	Calf length	402.28	27.03	467.5	342.5	mm
6	Knee width	96.66	8.22	124	74	mm
7	Foot length	245.47	15.31	281	210	mm
8	Height	1677.95	79.20	1865	1509	mm
9	Weight	58.56	9.33	98.6	37.5	kg

II. METHODOLOGY

A. Data Collection

We recruited 137 healthy adults (71 males and 66 females) from South China University of Technology (SCUT) in Guangzhou, China. None of them had any history of neurological injury or gait disorder. The experimental protocol was approved by the Ethics Committee of the Guangzhou First People's Hospital Department. Informed consent was obtained from all participants.

We measured 9 body parameters of each participant, as Fig. 1 and Table I show, age and gender were recorded through a questionnaire for each subject, and the other 7 body parameters were estimated by the experiment operator. For those parameters that exist on both the left and right sides of the body, we took the mean values. Table I shows the distribution of the collected body parameters.

Gait patterns were recorded with a Vicon motion capture system (Fig. 2) with 10 infrared cameras and 4 force plates. First, as shown in Fig. 3, we attached 16 reflective markers

[1]The values of gender are not applicable due to its discrete characteristic.

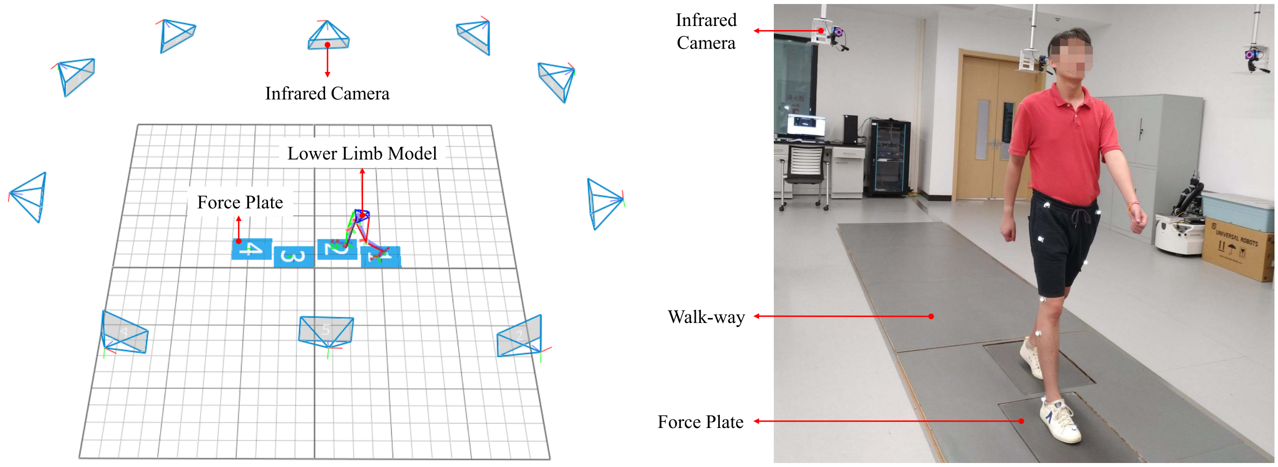

(a) Virtual Scene (b) Reality Scene

Fig. 2. Vicon motion capture system, consisting of 10 infrared cameras and 4 force plates. The sampling rates of the cameras and force plates are set to 250 Hz and 1000 Hz respectively. The cameras capture the movement of the markers that are used to reconstruct a lower limb model for calculating joint kinematics; force plates record the reaction force between the foot and ground to measure the foot-ground contact timings.

Fig. 3. Reflective markers attached to the subject.

to the subject, the marker positions are described in reference [27]. Then, we asked the experiment participants to walk 20 times on a 10 meter walkway at self-paced walking speed at five different speed levels. Meanwhile, the Vicon system measured the trajectories of the 16 reflective markers, which were used to calculate joint kinematics.

To keep the gait pattern natural, we did not ask subjects to intentionally step their foot fully on the force plates, even though data would be valid only in that case, so many collected gait patterns are not valid since heel strike moments cannot be measured.

Gait patterns are represented by lower limb joint trajectories: hip flexion/extension, knee flexion/extension, and ankle flexion/extension in the sagittal plane. Since most of the rehabilitation robots only support these three freedom of motion mentioned above, we decided to focus on these rotations in the sagittal plane.

TABLE II

MEAN AND STANDARD DEVIATION OF THE CALCULATED GAIT PARAMETERS FROM 4,425 COLLECTED GAIT PATTERNS

Parameter	Mean	Std	Max	Min	Unit
Walking speed	1.15	0.24	2.00	0.25	m/s
Stride length	1.30	0.11	1.71	0.15	m

B. Preprocessing of Collected Data

To obtain a well-organized data set and to speed up neural network training, raw gait data obtained from the Vicon system and collected body parameters need to go through a series of further processes.

1) **Remove invalid gait patterns**: Due to marker occlusion or foot deviation from force plates, not every collected gait pattern is valid, so we need to eliminate those data.
2) **Low-pass filtering**: To reduce noise data in the raw signals, we apply a Butterworth low-pass filter whose cut-off frequency is 6 Hz, as suggested by references [19], [28]. Fig. 4 shows a comparison between raw and filtered gait patterns; it is clear that the filtered waveform is much smoother.
3) **Split the gait sequence into gait cycles**: Our goal is to generate gait cycles, so we need to divide the gait patterns into several gait cycles. The moment when the heel strikes a force plate is used as the cut-off point to divide gait cycles.
4) **Calculate gait parameters**: The walking speed and stride length are calculated from gait data. The distribution of walking speed and stride length is presented in Table II.
5) **Unify the gait cycle lengths**: All gait cycles are normalized to the same period length (80) using a time resampling method; in other words, all gait cycles are expressed as 80 discrete values.
6) **Input normalization**: To improve neural network performance and to speed up the training process, all input features (body parameters and gait parameters) are

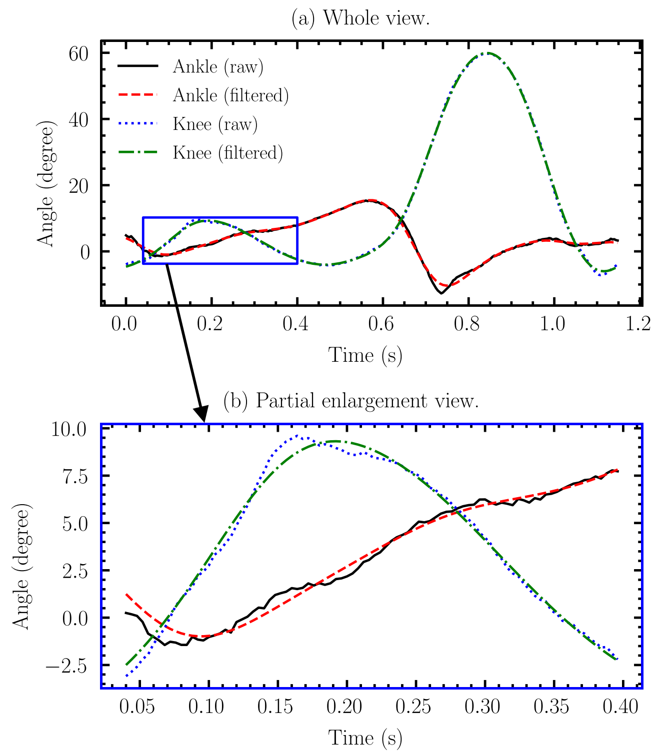

Fig. 4. Comparison between filtered and raw gait pattern. The curve of hip is not shown here for the sake of brevity.

normalized to a range between 0 and 1 using a Min-Max scaling method, which has wide application in machine learning (Equation 1).

$$x^k_{scaled} = \frac{x^k - min(x^k)}{max(x^k) - min(x^k)} \tag{1}$$

where k is the index of input feature.

Finally, we obtained a well structured data set containing 4,425 valid gait cycles from 137 subjects.

Algorithm 1 Forward Propagation of the GRU

Require: Sequence $\{\boldsymbol{x}_1, \boldsymbol{x}_2, \ldots, \boldsymbol{x}_n\}$;
Ensure: Sequence $\{\boldsymbol{y}_1, \boldsymbol{y}_2, \ldots, \boldsymbol{y}_n\}$;
  $h_0 \leftarrow 0$
  for $t = 1$ to n **do**
    Update gate: $z_t = \sigma(\boldsymbol{W}^z\boldsymbol{x}_t + \boldsymbol{U}^z\boldsymbol{h}_{t-1} + \boldsymbol{b}^z)$;
    Reset gate: $r_t = \sigma(\boldsymbol{W}^r\boldsymbol{x}_t + \boldsymbol{U}^r\boldsymbol{h}_{t-1} + \boldsymbol{b}^r)$;
    Candidate activation: $\tilde{\boldsymbol{h}}_t = tanh(\boldsymbol{W}\boldsymbol{x}_t + \underset{\sim}{r_t} \odot \boldsymbol{U}\boldsymbol{h}_{t-1})$;
    Activation: $\boldsymbol{h}_t = (1 - z_t) \odot \boldsymbol{h}_{t-1} + z_t \odot \tilde{\boldsymbol{h}}_t$;
    Output: $\boldsymbol{y}_t = tanh(\boldsymbol{V}\boldsymbol{h}_t)$;
  end for

where $\odot$ represents element-wise production, $\boldsymbol{W}$, $\boldsymbol{U}$, and $\boldsymbol{V}$ denote weights that are determined through optimization; $\boldsymbol{b}$ denotes biases; $\sigma(z) = \frac{1}{1+e^{-z}}$ is sigmoid activation function; $tanh(z) = \frac{e^z - e^{-z}}{e^z + e^{-z}}$ is tanh activation.

C. Gait Pattern Generation Model

We use a Gated Recurrent Unit (GRU)-based Recurrent Neural Network (RNN) as our gait generator, which takes body parameters and gait parameters as input and outputs gait patterns. RNNs are highly efficient neural networks designed for modeling sequence data such as sentences, voices, and gait patterns. RNNs are naturally more suitable for gait generation tasks than traditional feed-forward neural networks and have been widely used in gait classification [29], [30] and motion forecasting [31], [32].

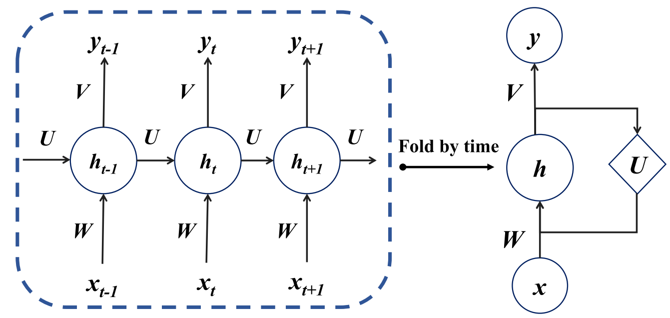

Fig. 5. A simple RNN, before and after folding by time.

The term *recurrent* means that the output of the RNN at the current time step will be part of the input to the next time step. As shown in Fig. 5, the hidden state $\boldsymbol{h}$ of an RNN is updated according to the current and previous states of the sequential inputs. In this way, the RNN considers not only the current input but also what it remembers about its previous elements.

Because traditional RNNs suffer from the gradient vanishing problem, our RNN model uses the GRU [33], [34], a variant of the traditional RNN, as its main structure. To restrain gradient vanishing, the GRU is designed with a reset gate that decides what to "forget" and an update gate that decides what to "remember". Alogorithm 1 demonstrates the forward propagation of the GRU.

Fig. 6 is the architecture of our RNN model, which consists of one GRU and 2 fully connected layers. For each time step of total 80 steps, the same input (body parameters and gait parameters) is passed to the RNN, which then outputs the corresponding joint angle at the current time step. That is, in Alogorithm 1, all the vectors in the input sequence are the same, $x_1 = x_2 = \ldots = x_n$.

The RNN is trained with Adam, an algorithm for first-order gradient-based optimization of stochastic objective functions [35]. We created and verified the RNN using Keras [36]. The activation function of the GRU unit and the first fully-connected layer is ReLU(Equation 2), the activation function of the second fully-connected layer is linear activation(Equation 3); their definitions are shown below:

$$ReLU(x) = \begin{cases} x, & \text{if } x \geq 0; \\ 0, & \text{otherwise.} \end{cases} \tag{2}$$

$$linear(x) = x; \tag{3}$$

The loss function of the RNN has two parts (Equation 4), one is the mean squared error (Equation 5), the other is the gap loss (Equation 6). The gap loss is designed to punish the RNN for generating non-periodic gait patterns.

$$Loss = Loss_{MSE} + Loss_{gap} \tag{4}$$

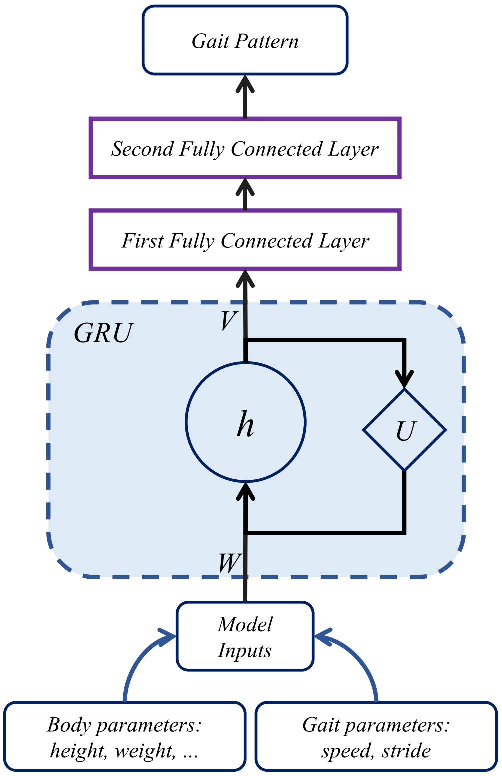

Fig. 6. The structure of the RNN. The model input vector includes 9 body parameters (Fig. 1) and 2 gait parameters (walking speed and stride length). Neurons in the first fully connected layer use ReLU activation(Equation 2); in the second layer, we apply linear activation(Equation 3). The loss function is mean squared error(Equation 5). Note that for each time step, the same input vector is passed to the RNN.

$$Loss_{MSE} = \frac{1}{TM}\sum_{i=1}^{M} \|\hat{\boldsymbol{y}}_i - \boldsymbol{y}_i\|_2 \tag{5}$$

$$Loss_{gap} = \frac{1}{M}\sum_{i=1}^{M} \left|\hat{\boldsymbol{y}}_{i,t=1} - \boldsymbol{y}_{i,t=80}\right| \tag{6}$$

where M is the number of samples in a training batch, T is the length of gait cycles (80 in specific), $\boldsymbol{y}_i$ is the actual gait pattern vector, and $\hat{\boldsymbol{y}}_i$ is the generated gait pattern vector.

III. Results

A. Verification of Generated Gait Patterns

We present a case study to demonstrate the similarity between the generated and actual gait patterns. We selected two representative subjects, no. 1 and no. 2, and their body parameters are shown in Fig. 7. Subject no. 1 has body parameters close to the mean values, whereas subject no. 2 deviates greatly from the mean values. Fig. 8 illustrates the generated and actual gait patterns of these subjects. Generally, the generated gait pattern of subject no. 1 is close to the actual gait; in most of the time, the deviation between the generated and actual gait is smaller than one std. However, the predicted ankle and hip patterns of subject no. 2 occasionally deviate from the actual patterns by more than one std, and we suppose that this is because subject no. 2's body parameters highly deviate from the average values.

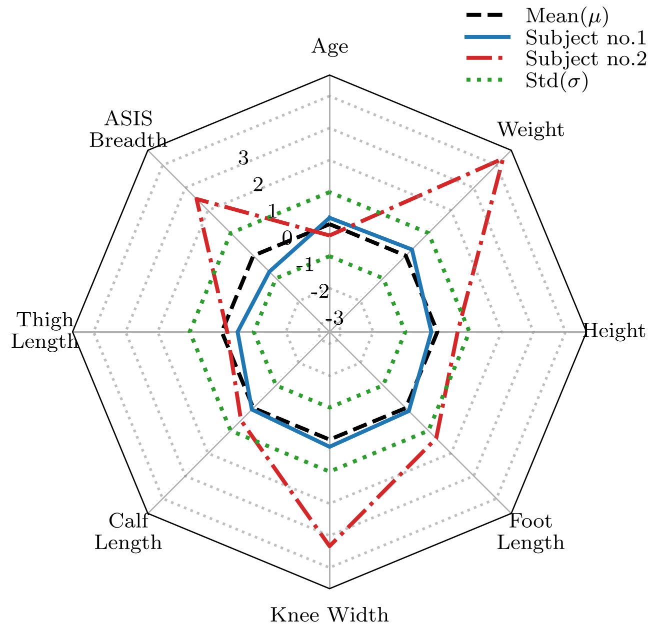

Fig. 7. The distribution of the body parameters of subject no. 1 (male) and subject no. 2 (male). All body features are normalized, so 0 indicates the mean value (μ), whereas 1 indicates one standard deviation (σ).

We verified the performance of our RNN model by comparing it with previous methods which have the same objective as ours [18], [19], all methods are applied to the same data set. We used the leave-one-subject-out cross-validation method to verify the performance of our RNN in gait generation, for each iteration, we randomly selected the data of one subject as the test set and the data of the remaining 136 subjects as the training set. Then, we trained the models on the training set and calculated the mean absolute deviation (MAD) of the models on the test set. And finally, we took the average MAD of these 137 iterations as the final result. The definition of MAD is given by Equation 7:

$$MAD = \frac{1}{TN}\sum_{i=1}^{N} \|\hat{\boldsymbol{y}}_i - \boldsymbol{y}_i\|_1 \tag{7}$$

where N is the number of samples in the test set, T is the length of gait cycles (80 in specific) and $\hat{\boldsymbol{y}}_i$ and $\boldsymbol{y}_i$ are the generated and actual gait patterns, respectively.

As shown in Fig. 9, our method achieved a significant precision improvement on the quality of the generated gait pattern. For the ankle, knee, and hip, our method has 12.83%, 20.95%, and 28.25% less MAD than the previous state-of-the-art method GRNN [19], respectively. Table III provides the details of the results.

B. Generating Gait Patterns at Continuously Varying Walking Speeds and Stride Lengths

Our RNN model is able to generate gait patterns at continuously varying walking speeds and stride lengths. To verify these properties, we created a virtual subject whose body parameters are set to the mean values of the 137 subjects, and we then generated gait patterns for this virtual subject at

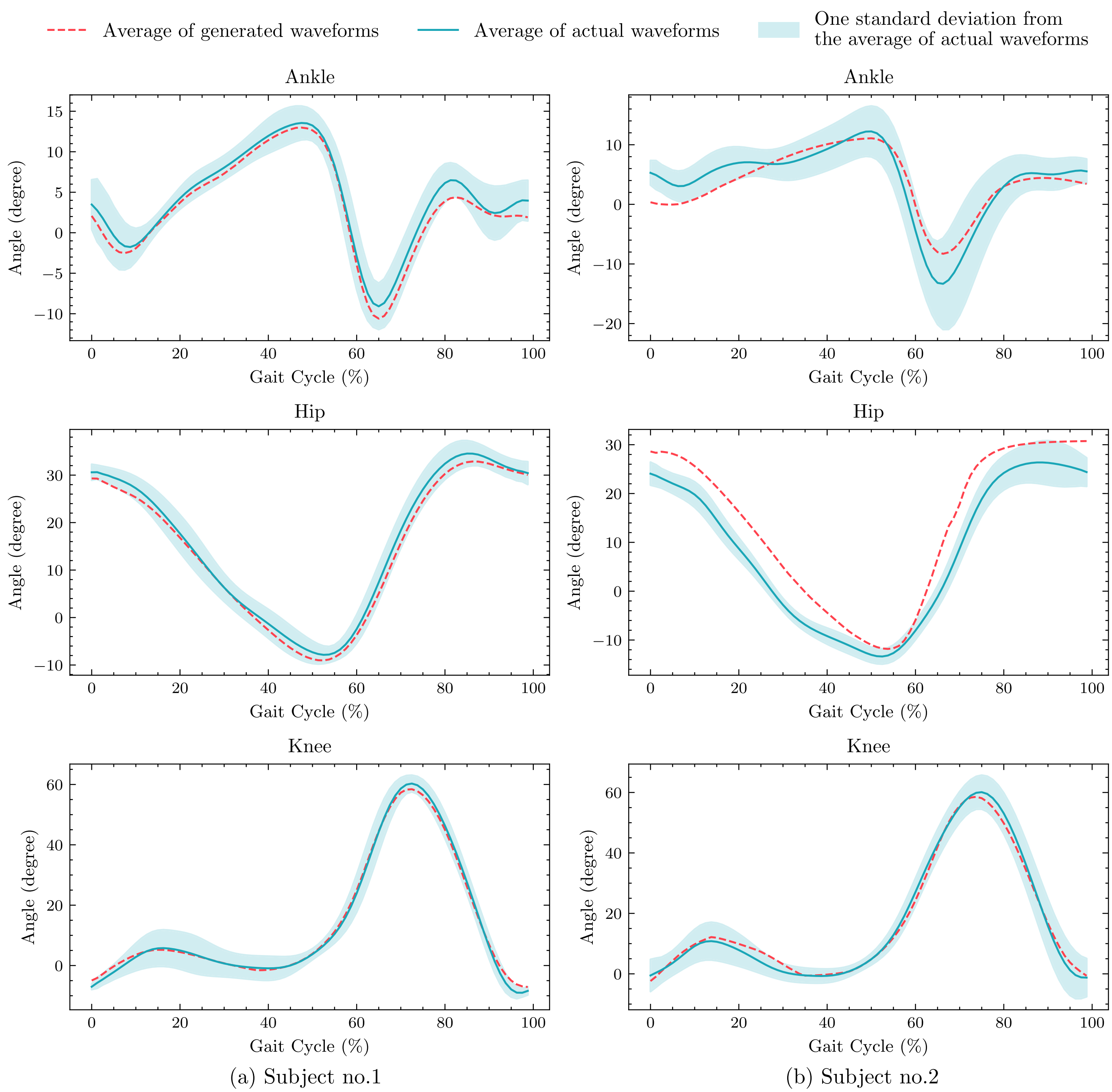

Fig. 8. Generated gait pattern vs actual gait pattern.

TABLE III
MAD(STD) COMPARISON AMONG METHODS (IN DEGREES)

Joint	RNN	GRNN	GPR
Ankle	3.60(1.49)	4.13(1.84)	4.36(1.92)
Knee	4.98(2.12)	6.30(2.50)	6.31(2.47)
Hip	4.57(3.25)	6.37(4.16)	6.33(4.17)

varying walking speeds and stride lengths. Fig. 10 shows the generated patterns at a walking speed ranging from 0.85 m/s to 1.05 m/s at an interval of 0.05 m/s, and the gait is updated smoothly when increasing walking speed is input into the gait generation model. The plots also illustrate that the peaks of the hip and knee joint are increased when the walking speed is increased, which agrees with a previous study of gait kinematics [37]. Fig. 11 shows the generated gait patterns at stride lengths ranging from 1.10 m to 1.30 m at intervals of 0.05 m, and the connections between the gait patterns with different stride lengths are smooth. These results indicated that our method is able to generate gait patterns during self-paced walking.

C. Periodicity of Generated Gait Patterns

The periodicity of the reference gait is very important for the lower limb rehabilitation robot. If the generated gait patterns are not periodic, for example, a significant gap between the beginning and the end of the joint trajectory, this will lead

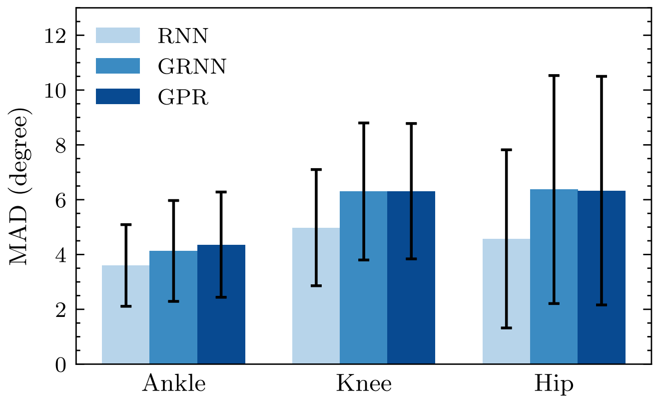

Fig. 9. MAD (std) measured in different methods. GRNN and GPR are proposed in [19] and [18] respectively.

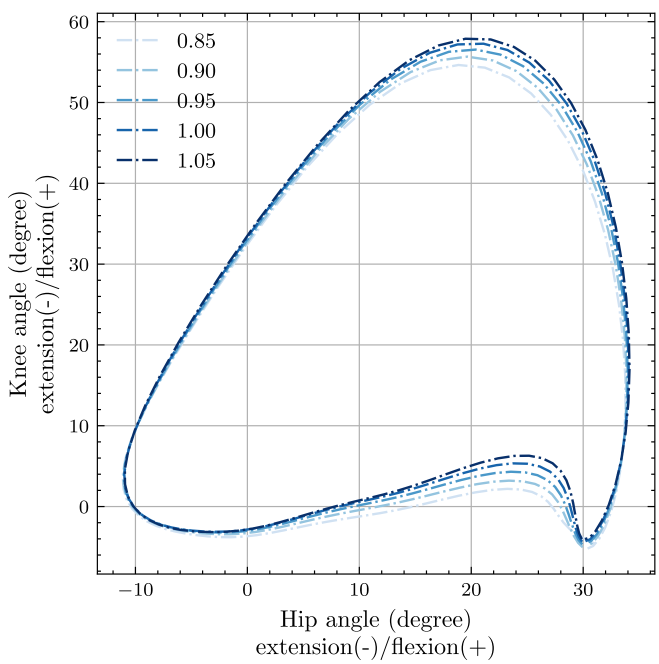

Fig. 10. Cyclogram of gait patterns generated in the walking speed range 0.85 to 1.05m/s at intervals of 0.05m/s.

TABLE IV
AVERAGE GAP COMPARISON (IN DEGREES)

Joint	GRNN	RNN with gap loss	RNN without gap loss
Ankle	0.66	0.46	2.81
Knee	0.47	0.52	2.24
Hip	0.34	0.65	2.58

to a jerky behavior of the rehabilitation robot. In order to solve this problem, we added the gap loss (Equation 6) to the loss function of the RNN. In this way, the RNN will try to minimize the discontinuity between the initial state and the ending state. After adding the gap loss, the discontinuity of the generated gait is well inhibited. As shown in Fig. 12 and Table IV, the average gap between the beginning and the end of generated gait patterns dropped a lot after adding the gap loss term to the loss function. The performance of our method

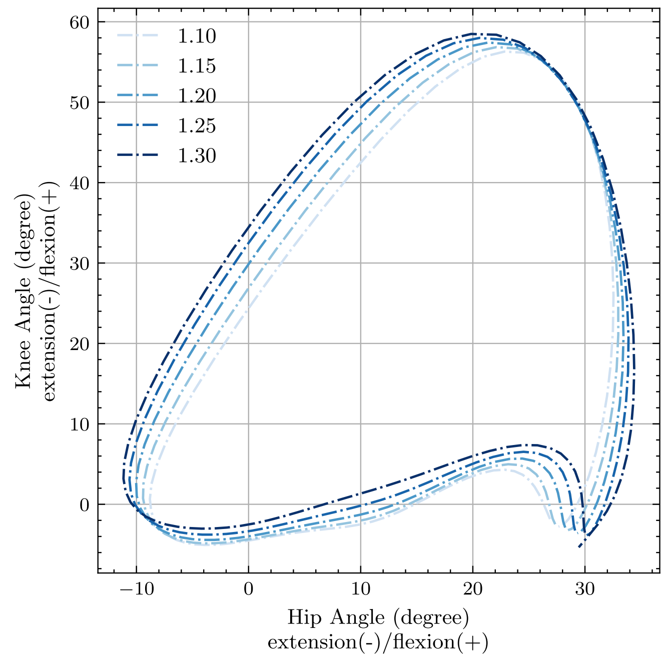

Fig. 11. Cyclogram of gait patterns generated in the stride length range 1.10 to 1.30m at intervals of 0.05m.

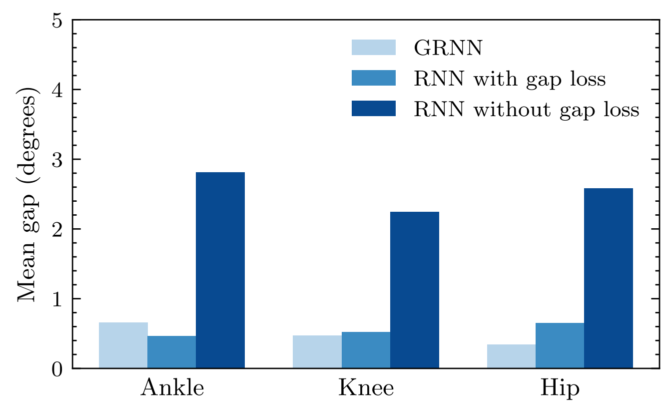

Fig. 12. Average gap comparison.

on generating periodic gait patterns is close to the GRNN with periodic basis functions.

IV. DISCUSSION

A. Mean Error of Generated Gait Pattern

What value of the prediction error would be low enough for our intended application? Some gait rehabilitation robots ([4], [5]) select reference gait from a large gait data set(e.g. CGA database [28]). For example, selecting the gait patterns of a healthy subject whose body parameters are close to the patient as the reference gait pattern. Reference [19] reported that the MAD values of the CGA method are 6.03, 9.28, and 7.66 for ankle, knee, and hip respectively. The CGA method has been widely tested that it can achieve effective rehabilitation training, thus it is proper to accept the MAD values of the CGA method as the threshold values, any value below this threshold would be enough for our intended application. It is obvious that our RNN model produces much less error than the CGA method.

B. Walking Speed and Stride Length

In different stages of the gait rehabilitation process, the rehabilitation robotic system needs to control the walking of patients at different speeds. For instance, in the early stages of recovery, a lower walking speed is required since the motor ability of the patient is still low. As the patient recovers their walking ability, gait velocity should be increased for a better rehabilitation effect. Nevertheless, many previous works only produce gait at a single fixed speed [12], [18] or several speeds [20], [21]. In contrast, our method is able to generate gait patterns at continuously varying walking speeds (Fig. 10), which provides a better rehabilitation effect since self-paced walking is enabled.

Stride length is another important gait parameter. Espy *et al.* [25] showed that a smaller stride increases walking stability, which is beneficial to hemiplegia patients. Thus, it is meaningful to plan gait at a smaller stride for rehabilitation robots, and the experimental results demonstrated that our method is capable of achieving that (Fig. 11).

C. Regression Model

The effectiveness of our approach can be attributed to the high fitting efficiency of the RNN. Due to the high dimensionality of gait data, it is difficult for regression models with small complexity to fit gait patterns properly. Many previous works have to use dimensionality reduction methods, such as Fourier transforms [19] or GPDM [21] to encode gait into a smaller dimension. However, dimensionality reduction leads to unavoidable reconstruction errors. As a highly efficient nonlinear fitting model, our RNN can fit the gait pattern perfectly, and there is no need for dimension reduction. Also, the RNNs are specially designed for modeling time series such as gait patterns, this makes them extremely suitable for the gait generation task. We believe this is the main reason for the outstanding performance of our RNN. Unfortunately, the dilemma is that the RNN often overfits, which requires us to use a larger data set and take other actions to prevent over-fitting.

D. Limitations

There are still some limitations in our work. First, the RNN is a so-called "black box" model; although it achieved an excellent fit, it cannot help us obtain any underlying relation between body parameters and gait patterns. This applies to all statistical methods including GPR and GRNN. The second limitation is that the model does not handle the asymmetry of the gait patterns and body parameters well. For those body parameters that can be measured on both sides of the body, such as thigh length and foot length, we take the average value. We did not create different gaits for the left and right sides of the lower limbs, and in doing so, we ignored the asymmetry of the joint kinematics of both sides.

V. Conclusion

This paper presented a novel gait generation method based on recurrent neural networks. The generated subject-specific gait pattern can be used as a reference gait for lower limb rehabilitation robots to provide a better rehabilitation effect. We collected and cleaned the largest gait data set, which contains 4,425 gait patterns from 137 subjects and the corresponding body parameters. Using this data set, we trained a recurrent neural network as our gait generation model, which takes the body parameters of a subject and desired gait parameters as input and outputs a gait pattern that is tailored to the subject. We evaluated our model using leave-one-subject-out cross-validation. The results showed that our method is able to generate subject-specific gait patterns at self-paced walking speeds and strides with the lowest error among all works.

References

[1] D. R. Louie and J. J. Eng, "Powered robotic exoskeletons in post-stroke rehabilitation of gait: A scoping review," *J. Neuroeng. Rehabil.*, vol. 13, no. 1, pp. 1–10, Dec. 2016.

[2] L. J. Holanda, P. M. M. Silva, T. C. Amorim, M. O. Lacerda, C. R. Simão, and E. Morya, "Robotic assisted gait as a tool for rehabilitation of individuals with spinal cord injury: A systematic review," *J. Neuroeng. Rehabil.*, vol. 14, no. 1, pp. 1–7, Dec. 2017.

[3] J. F. Veneman, R. Kruidhof, E. E. G. Hekman, R. Ekkelenkamp, E. H. F. Van Asseldonk, and H. van der Kooij, "Design and evaluation of the LOPES exoskeleton robot for interactive gait rehabilitation," *IEEE Trans. Neural Syst. Rehabil. Eng.*, vol. 15, no. 3, pp. 379–386, Sep. 2007.

[4] S. K. Banala, S. H. Kim, S. K. Agrawal, and J. P. Scholz, "Robot assisted gait training with active leg exoskeleton (ALEX)," *IEEE Trans. Neural Syst. Rehabil. Eng.*, vol. 17, no. 1, pp. 2–8, Feb. 2009.

[5] Y. Stauffer *et al.*, "The WalkTrainer—A new generation of walking reeducation device combining orthoses and muscle stimulation," *IEEE Trans. Neural Syst. Rehabil. Eng.*, vol. 17, no. 1, pp. 38–45, Feb. 2009.

[6] R. Riener, L. Lünenburger, I. Maier, G. Colombo, and V. Dietz, "Locomotor training in subjects with sensori-motor deficits: An overview of the robotic gait orthosis lokomat," *J. Healthcare Eng.*, vol. 1, no. 2, pp. 197–216, Jun. 2010.

[7] S. Wang *et al.*, "Design and control of the MINDWALKER exoskeleton," *IEEE Trans. Neural Syst. Rehabil. Eng.*, vol. 23, no. 2, pp. 277–286, Mar. 2015.

[8] B. French *et al.*, "Does repetitive task training improve functional activity after stroke? A Cochrane systematic review and meta-analysis," *J. Rehabil. Med.*, vol. 42, no. 1, pp. 9–15, 2010.

[9] K. Scrivener, C. Sherrington, and K. Schurr, "Exercise dose and mobility outcome in a comprehensive stroke unit: Description and prediction from a prospective cohort study," *J. Rehabil. Med.*, vol. 44, no. 10, pp. 824–829, 2012.

[10] A. Kale *et al.*, "Identification of humans using gait," *IEEE Trans. Image Process.*, vol. 13, no. 9, pp. 1163–1173, Sep. 2004.

[11] R. L. McGrath, M. Pires-Fernandes, B. Knarr, J. S. Higginson, and F. Sergi, "Toward goal-oriented robotic gait training: The effect of gait speed and stride length on lower extremity joint torques," in *Proc. Int. Conf. Rehabil. Robot. (ICORR)*, Jul. 2017, pp. 270–275.

[12] S. Ren *et al.*, "Personalized gait trajectory generation based on anthropometric features using random forest," *J. Ambient Intell. Humanized Comput.*, Jul. 2019, doi: 10.1007/s12652-019-01390-3.

[13] H. Vallery, E. H. F. van Asseldonk, M. Buss, and H. van der Kooij, "Reference trajectory generation for rehabilitation robots: Complementary limb motion estimation," *IEEE Trans. Neural Syst. Rehabil. Eng.*, vol. 17, no. 1, pp. 23–30, Feb. 2009.

[14] F. C. Anderson and M. G. Pandy, "Dynamic optimization of human walking," *J. Biomech. Eng.*, vol. 123, no. 5, pp. 381–390, Oct. 2001.

[15] Y. Xiang, J. S. Arora, S. Rahmatalla, and K. Abdel-Malek, "Optimization-based dynamic human walking prediction: One step formulation," *Int. J. Numer. Methods Eng.*, vol. 79, no. 6, pp. 667–695, Feb. 2009.

[16] Y. Xiang, J. S. Arora, and K. Abdel-Malek, “Optimization-based prediction of asymmetric human gait,” *J. Biomech.*, vol. 44, no. 4, pp. 683–693, Feb. 2011.

[17] H. B. Lim, T. P. Luu, K. H. Hoon, and K. H. Low, “Natural gait parameters prediction for gait rehabilitation via artificial neural network,” in *Proc. IEEE/RSJ Int. Conf. Intell. Robots Syst. (IROS)*, Oct. 2010, pp. 5398–5403.

[18] Y. Yun, H.-C. Kim, S. Y. Shin, J. Lee, A. D. Deshpande, and C. Kim, “Statistical method for prediction of gait kinematics with Gaussian process regression,” *J. Biomech.*, vol. 47, no. 1, pp. 186–192, Jan. 2014.

[19] T. P. Luu, K. H. Low, X. Qu, H. B. Lim, and K. H. Hoon, “An individual-specific gait pattern prediction model based on generalized regression neural networks,” *Gait Posture*, vol. 39, no. 1, pp. 443–448, Jan. 2014.

[20] X. Wu, D.-X. Liu, M. Liu, C. Chen, and H. Guo, “Individualized gait pattern generation for sharing lower limb exoskeleton robot,” *IEEE Trans. Autom. Sci. Eng.*, vol. 15, no. 4, pp. 1459–1470, Oct. 2018.

[21] J. Hong, C. Chun, S.-J. Kim, and F. C. Park, “Gaussian process trajectory learning and synthesis of individualized gait motions,” *IEEE Trans. Neural Syst. Rehabil. Eng.*, vol. 27, no. 6, pp. 1236–1245, Jun. 2019.

[22] D.-X. Liu, X. Wu, W. Du, C. Wang, C. Chen, and T. Xu, “Deep spatial-temporal model for rehabilitation gait: Optimal trajectory generation for knee joint of lower-limb exoskeleton,” *Assem. Autom.*, vol. 37, no. 3, pp. 369–378, Aug. 2017.

[23] S. J. Olney and C. Richardsb, “Hemiparetic gait following stroke. Part I: Characteristics,” *Gait Posture*, vol. 4, no. 2, pp. 136–148, 1996.

[24] M. H. Schwartz, A. Rozumalski, and J. P. Trost, “The effect of walking speed on the gait of typically developing children,” *J. Biomech.*, vol. 41, no. 8, pp. 1639–1650, 2008.

[25] D. D. Espy, F. Yang, T. Bhatt, and Y.-C. Pai, “Independent influence of gait speed and step length on stability and fall risk,” *Gait Posture*, vol. 32, no. 3, pp. 378–382, Jul. 2010.

[26] Y. Huang *et al.*, “The effects of stride length and stride frequency on trunk coordination in human walking,” *Gait Posture*, vol. 31, no. 4, pp. 444–449, Apr. 2010.

[27] Vicon Motion Systems Ltd., “Plug-in gait reference guide,” Vicon Motion Syst. Ltd., Yarnton, U.K., Tech. Rep., 2016.

[28] D. A. Winter, *Biomechanics and Motor Control of Human Movement*. Hoboken, NJ, USA: Wiley, 2004.

[29] M. Khokhlova, C. Migniot, A. Morozov, O. Sushkova, and A. Dipanda, “Normal and pathological gait classification LSTM model,” *Artif. Intell. Med.*, vol. 94, pp. 54–66, Mar. 2019.

[30] K. Jun, D.-W. Lee, K. Lee, S. Lee, and M. S. Kim, “Feature extraction using an RNN autoencoder for skeleton-based abnormal gait recognition,” *IEEE Access*, vol. 8, pp. 19196–19207, 2020.

[31] E. Aertbelien and J. De Schutter, “Learning a predictive model of human gait for the control of a lower-limb exoskeleton,” in *Proc. 5th IEEE RAS/EMBS Int. Conf. Biomed. Robot. Biomechatronics*, Aug. 2014, pp. 520–525.

[32] A. Zaroug, D. T. H. Lai, K. Mudie, and R. Begg, “Lower limb kinematics trajectory prediction using long short-term memory neural networks,” *Frontiers Bioeng. Biotechnol.*, vol. 8, pp. 1–12, May 2020.

[33] C. Gulcehre, K. Cho, R. Pascanu, and Y. Bengio, “Learned-norm pooling for deep feedforward and recurrent neural networks,” in *Proc. Joint Eur. Conf. Mach. Learn. Knowl. Discovery Databases*, in Lecture Notes in Computer Science: Including Subseries Lecture Notes in Artificial Intelligence and Lecture Notes in Bioinformatics, vol. 8724, 2014, pp. 530–546. [Online]. Available: http://arxiv.org/abs/1311.1780

[34] J. Chung, C. Gulcehre, K. Cho, and Y. Bengio, “Empirical evaluation of gated recurrent neural networks on sequence modeling,” Apr. 2014, *arXiv:1412.3555*. [Online]. Available: http://arxiv.org/abs/1412.3555

[35] D. P. Kingma and J. L. Ba, “Adam: A method for stochastic optimization,” in *Proc. 3rd Int. Conf. Learn. Represent. (ICLR)*, 2015, pp. 1–15.

[36] F. Chollet. (2015). *Keras*. [Online]. Available: https://keras.io

[37] C. A. Fukuchi, R. K. Fukuchi, and M. Duarte, “Test of two prediction methods for minimum and maximum values of gait kinematics and kinetics data over a range of speeds,” *Gait Posture*, vol. 73, pp. 269–272, Sep. 2019.